Research Article | Vol. 26, No. 24 | 26 Nov 2018 | OPTICS EXPRESS 32055
Optics EXPRESS

Free-space coupling enhancement of micro-resonators via self-accelerating beams

XU LIU,[1] YI HU,[1*] PENGBO JIA,[1] PING ZHANG,[1] HAO WU,[1] ZHENZHONG HAO,[1] FANG BO,[1] ZHIGANG CHEN,[1,2] AND JINGJUN XU[1,3]

[1]*The MOE Key Laboratory of Weak-Light Nonlinear Photonics, TEDA Applied Physics Institute and School of Physics, Nankai University, Tianjin 300457, China*
[2]*zgchecn@nankai.edu.cn*
[3]*jjxu@nankai.edu.cn*
**yihu@nankai.edu.cn*

Abstract: We study free-space coupling of optical fields to the whispering-gallery-mode resonators by employing self-accelerating beams orbiting a semicircle. The best coupling condition is obtained through theoretical analysis, in accord with the numerical results. Comparing with the conventional Gaussian-like beams, much enhanced coupling efficiency is achieved with such self-accelerating beams, particularly when a large numerical aperture of an optical system is used or a higher-order azimuthal mode is considered. Conditions with slight deviation from the ideal radius of self-accelerating beams are further discussed, aiming to realize an optimized high coupling efficiency.

1. Introduction

Whispering-gallery-mode (WGM) resonators, featured with a high-quality factor and a small mode volume, have attracted an increased attention in optics and photonics, fueled by their potential applications in sensor, low-power lasing, frequency comb generation, optomechanics and so on [1–4]. Thus far, efficient coupling to these devices can be realized by properly positioning a fiber taper or a prism closely near them [5]. However, the targets are prone to be reshaped upon any mechanical contact when they are droplets (made of liquid or soft matters). Moreover, some biological measurements in liquid environments may face difficulties on the bulky alignment of these evanescent couplers, as well as on some unexpected background signals coming from the coupler susceptible to contamination [6–8]. In these scenarios, free-space coupling is desirable, via matching between the WGMs and an illuminated field, as it has advantages in terms of alignment as well as maintenance of droplet integrity [8]. Unfortunately, free-space coupling is typically afflicted with low coupling efficiency when Gaussian-like beams are used, mismatched with the WGMs of circular symmetry [9]. To solve this problem, deformed resonators were put forward aiming to break the rotational symmetry [10–16]. This approach faces the degradation of Q factor, however, and becomes complicated if one tries to apply it to droplets. As an alternative approach, scatters placed in the field of WGM are introduced to couple a far field light into the resonator, but the manipulation on these scatters increases the complexity of the associated setups [17,18].

Recently, a new kind of beams, namely self-accelerating beams, has attracted lots of attention [19–21]. By merely altering the wavefront of a plane wave, the generated beams can propagate along a designed trajectory in free space. In particular, these beams can be designed to propagate following a half circle [22–24], where the field in the polar direction is described by a Bessel function. Such a kind of beams is named as “half-Bessel self-accelerating beams”. Their field distributions are much closer to that of the WGM than the Gaussian-like beams, leading to possible enhancement of free space coupling.

#347095 https://doi.org/10.1364/OE.26.032055
Journal © 2018 Received 15 Oct 2018; revised 13 Nov 2018; accepted 15 Nov 2018; published 19 Nov 2018

Optics EXPRESS

In this Letter, we study free space coupling to the WGM resonators by employing the self-accelerating beams propagating along a semicircle path. Via theoretical analysis, the best coupling condition is obtained, which is in good agreement with that obtained from numerical simulations. The influence of the numerical aperture of an optical system for generating these beams with different radii of the semicircle is further discussed. Comparing with the illumination of Gaussian-like beams, self-accelerating beams exhibit a much enhanced coupling efficiency.

2. Theoretical model

Our target resonator is a dielectric cylinder with a refractive index n = 1.45 and a radius R = 10 μm and without considering its absorption and surface roughness, and the analysis on this model can be simplified into a two-dimensional coordinate where the origin is set to coincide with the cavity center as shown in Fig. 1. In this configuration, for the steady state (here consider the TM mode, and our following analysis can also apply to case of TE mode) in the resonator illuminated by an optical beam, the field distribution E_z inside and outside the cavity can be assumed in the following form in polar coordinates (r, ϕ) [9]:

$$\begin{cases} E_{zi} = \sum_m a_m J_m(nkr)\exp(im\phi) \quad (r \le R), \\ E_{zo} = \sum_m \left[b_m H_m^{(1)}(kr) + c_m H_m^{(2)}(kr) \right] \exp(im\phi) \quad (r > R), \end{cases} \tag{1}$$

where k is the vacuum wave number, J_m is the Bessel function of the 1st kind, and $H_m^{(1)}$ and $H_m^{(2)}$ are Hankel functions of the 1st and 2nd kinds, corresponding to the outgoing and incoming parts of the field outside the resonator, respectively. The coefficient c_m associated with the incoming contribution is merely determined by matching degree between the illuminating optical field and the radiation of cavity modes, while the other two coefficients a_m and b_m can be calculated by solving Eq. (1) under the boundary condition, i.e., $E_{zi}(R) = E_{zo}(R)$, and $H_{\phi i}(R) = H_{\phi o}(R)$, where $H_\phi \propto \partial E_z/\partial r$. For comparison, both Gaussian-like beams and self-accelerating beams are employed to illuminate this cavity. Their locations are defined by the position corresponding to the peak intensity of the Gaussian-like beams and the center of the (half) circular trajectory for the accelerating beams, respectively (see Fig. 1).

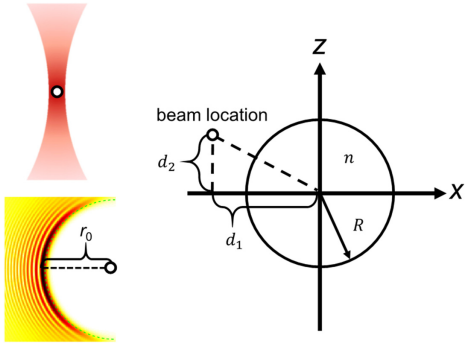

Fig. 1. Configuration of free-space coupling to a cylindrical resonator (right) via a Gaussian-like beam (top left) and a self-accelerating beam (bottom left), where the small empty circles mark the beam locations.

3. Results and discussion

In general, Gaussian-like beams and self-accelerating beams can be obtained by inputting a quasi-plane wave into a lens or an objective that can perform a Fourier transformation. Then the field distribution near the focus of either optical component can be written as:

Optics EXPRESS

$$E(x,z)=\frac{1}{\sqrt{P}}\int_{k_{x\min}}^{k_{x\max}} e^{i\left[k_x x+k_z z+\rho(k_x)\right]}dk_x, \tag{2}$$

where the range of integration is determined by the numerical aperture (NA) of the optical system, $P = 4\pi k^2 \cdot NA$ is a normalized factor to keep the input power as a constant, and $\rho(k_x)$ is a phase modulation imposed on the quasi-plane wave to generate the half-Bessel accelerating beams [25,26] as well as to modify the beam location, i.e.,

$$\rho(k_x)=-k_x d_1-k_z d_2+r_0 k\arcsin(k_x/k), \tag{3}$$

where d_1 and d_2 are the offsets imposed on the beam along horizontal and vertical directions as indicated in Fig. 1, and r_0 is the radius of the circle followed by the accelerating beams. If r_0 is zero, the phase modulation corresponds to a Gaussian-like beam. Equation (2) can be transformed into a format in a polar coordinate:

$$E(r,\phi)=\frac{1}{\sqrt{P}}\int_{\theta_{\min}}^{\theta_{\max}} e^{i\left[kr\cos(\theta-\phi)+\rho(\theta)\right]}d(k\sin\theta), \tag{4}$$

by using $k_x = k\sin\theta$, $k_z = k\cos\theta$, $x = r\sin\phi$ and $z = r\cos\phi$. Equation (4) can be further simplified as:

$$E(r,\phi)=\sum_{m=-\infty}^{+\infty} c_m J_m(kr)\exp(im\phi), \tag{5}$$

by employing the formula $\exp(it\sin\theta)=\sum J_m(t)\exp(im\theta)$. The light field evolution is then described on the basis of Bessel functions, and the coefficient of each component is:

$$c_m=\frac{1}{\sqrt{P}}\exp\left(i\frac{\pi}{2}m\right)\int_{\theta_{\min}}^{\theta_{\max}} e^{i\left[-m\theta+\rho(\theta)\right]}k\cos\theta d\theta. \tag{6}$$

For this cylindrical resonator, one resonant wavelength of light usually corresponds to a particular mode, say, the m'^{th} order mode. Therefore, the m'^{th} term in the incoming accelerating beam dominates the energy stored inside the cavity (indeed corresponding to a phase matching condition), and its modulus can reach the maximum when considering that the value of $\cos\theta$ is always positive in the range of integration. Then we can obtain

$$-k\sin\theta d_1-k\cos\theta d_2+(r_0 k-m')\theta=0. \tag{7}$$

To make the above equation always satisfied, the following condition should be met: $d_1 = 0$, $d_2 = 0$, and $r_0 k = m'$. Thus, to realize an optimal coupling, the radius of the half-Bessel accelerating beam should be set to be m'/k, and meanwhile the center of the circular path should overlap with that of the resonator, which basically leads to the best azimuthal mode matching.

Next, the coupling via accelerating beams is studied when the above optimal conditions are deviated. Firstly, we consider the position offsets, by employing the optimal radius fixed as m'/k. As a typical example, a mode with the 92th azimuthal order and the 4th radial order (corresponding to a resonant wavelength around 781.65 nm) of the cavity and an optical system with NA = 0.85 are under concern. The calculated $|c_{92}|^2$ by employing Eq. (6) is presented in Fig. 2(a). As expected from the analysis, this value reaches the maximum at d_1 = 0 and d_2 = 0, while it dramatically drops at an offset position, which is more apparent along the horizontal direction (say, in a range of several hundred nanometers). In contrast, there is a quite larger parametric space of d_1 and d_2 to let $|c_{92}|^2$ be close to its maximum for the Gaussian-like beams, particularly along the vertical direction [Fig. 2(b)]. The perfect mode

Optics EXPRESS

matching for the accelerating beams is much better than the Gaussian counterpart, indicating an enhanced coupling. Using the same parameters, we performed numerical modeling by means of the software COMSOL (note that the resonant wavelength corresponding to this mode shifts to ~780.04 nm as a result of the non-smooth cavity surface caused by mesh generation). The energy stored in the cavity is calculated for various locations of the incoming optical beam, and is presented in Figs. 2(c) and 2(d) for the accelerating beams and the Gaussian-like beams, respectively. They show the same tendency as the variance of $|c_{92}|^2$ in Figs. 2(a) and 2(b), verifying the validity of the analysis described by Eq. (6). Similar results are obtained when other order resonate modes are considered, and the associated optimal coupling conditions for the two kinds of beams will be revisited and compared later. Note that Eq. (6) is not dependent on the radius of the cavity. If one employs different radii, the results shown in Fig. 2 are reproduced in a scaled parameter space of (d_1, d_2).

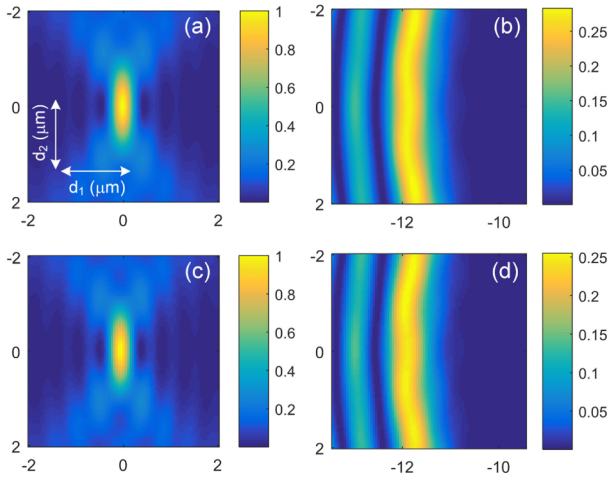

Fig. 2. Analysis of coupling efficiency to the microcavity (the quality factor is 3.216×10^5 for the mode under test) for (a,c) accelerating beams and (b,d) Gaussian-like beams as a function of different beam locations, characterized by (a, b) the calculated values of mode coefficients $|c_{92}|^2$ via Eq. (6), and (c, d) the computed energy in the resonator via COMSOL. The plotted values in (a,b) and (c,d) are normalized by the maximum value in (a) and (c), respectively.

Under the condition of optimal coupling, the distribution of c_m associated with the accelerating beam is shown in Fig. 3(a). It has a tight localization around the order $m' = 92$, and tends to become more localized when a larger NA is used. For comparison, the distribution of c_m associated with a Gaussian-like beam under one of the optimal coupling condition (i.e., $d_1 \approx$-11.7 μm, $d_2 \approx$-1.71 μm) is presented in Fig. 3(b). It spreads energy to many orders of Bessel components, and hence the weight on $m' = 92$ is reduced, indicating a less efficient coupling.

Optics EXPRESS

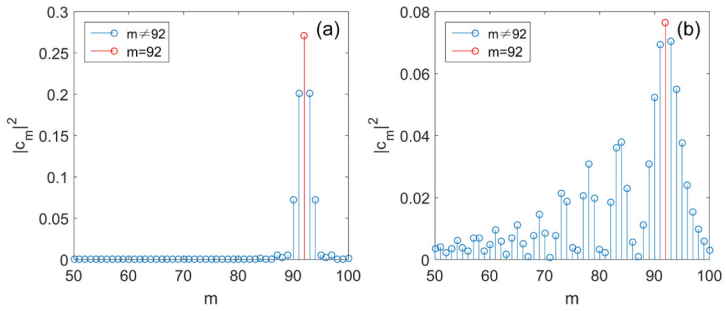

Fig. 3. The weight ($|c_m|^2$) of each Bessel component for the case of (a) the self-accelerating beam and (b) the Gaussian-like beam under the optimal coupling condition in Fig. 2, where *NA* = 0.85 is employed. Notice the difference in the *y*-axis scale.

In the following, we examine the influence of *NA* on the optimized coupling. Using Eqs. (6) and (7), one can obtain

$$\left|c_{m'}\right|^2_{optimal} = NA/\pi. \tag{8}$$

Thus the optimal coupling efficiency for the accelerating beams linearly increases with the *NA* yet it is independent of the mode order that is linked to the value of the quality factor. For the Gaussian-like beams, the largest value of $|c_{m'}|^2$ can be obtained by choosing proper values of d_1 and d_2 in Eq. (6), as presented in Fig. 4. In the limit of lower *NA* (i.e., $\sin\theta \sim\theta$), one can get the same results with Eq. (8) following a similar derivation. However, in the limit of larger *NA*, the Gaussian-like beams experience a tight focusing, less-matched with the resonating mode. For the Gaussian case, the coefficient $|c_{m'}|^2$ associated with the optimal coupling can reach the maximum when a proper *NA* is chosen, and this optimized *NA* tends to become smaller accompanying with a worse mode matching as a higher order azimuthal mode is considered. Therefore, in experiment, one should choose a proper *NA*, or choose a suitable beam size, aiming for the best free space coupling condition for the Gaussian case. Both ways bring complexity of the experiment. Nevertheless, the experimental conditions become much simpler for the case of accelerating beams to reach the best coupling efficiency, as long as a larger *NA* is employed. From Fig. 4, one can clearly see that the coupling via accelerating beams is greatly enhanced, and this enhancement is much more obvious for an optical system with a larger *NA*, or for the excitation of a higher order azimuthal mode (basically corresponding to a larger value of quality factor).

Optics EXPRESS

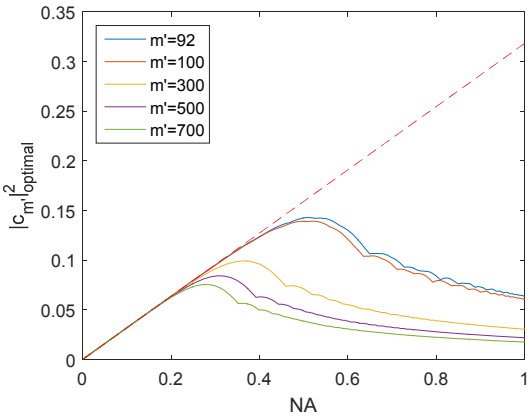

Fig. 4. Optimized value of $|c_{m'}|^2$ as a function of *NA* for accelerating beams (dashed line) and Gaussian-like beams (solid lines).

From the above analysis, one can infer that the only parameter to influence the optimal coupling efficiency of the accelerating beams is the radius. In the following study, we employ different radii to study the mode matching. If there is an offset (denoted as ε) to the ideal radius, the beam location should accordingly have a horizontal shift (denoted as α) to reach a good mode matching. Then Eq. (6) becomes:

$$c_m = \frac{1}{\sqrt{P}} \exp\left(i\frac{\pi}{2} m \right) \int_{\theta_{\min}}^{\theta_{\max}} e^{i(-k\sin\theta\alpha + \varepsilon k\theta)} k\cos\theta d\theta. \tag{9}$$

By expanding the exponential term of the above formula up to the 2nd order, we can obtain:

$$c_{m'} = \frac{1}{\sqrt{P}} \exp\left(i\frac{\pi}{2} m' \right) \left(2k\sin\theta_{\max} + A\alpha^2 + B\alpha + C \right), \tag{10}$$

where

$$\begin{aligned} A &= -k^3 \sin^3\theta_{\max} / 3, \\ B &= \left[\sin(2\theta_{\max}) - 2\theta_{\max}\cos(2\theta_{\max}) \right] k^3\varepsilon / 4, \\ C &= -k^3 \left[\left({\theta_{\max}}^2 - 2 \right) \sin\theta_{\max} + 2\theta_{\max}\cos\theta_{\max} \right] \varepsilon^2, \end{aligned} \tag{11}$$

Thus, the maximum of $|c_{m'}|^2$ appears at $\alpha = s\varepsilon$, where

$$s = 3\left[\sin(2\theta_{\max}) - 2\theta_{\max}\cos(2\theta_{\max}) \right] / \left(8\sin^3\theta_{\max} \right), \tag{12}$$

which indicates that the beam location should be linearly shifted with the change of radius aiming for the optimized coupling, as shown by the case of m' = 92 in Fig. 5(a). The associated slope *s* monotonically increases with *NA* from an initial value of 1 [Fig. 5(b)]. Above ~96% of the ideal coupling efficiency (characterized via Eq. (8)) can be maintained when the radius has an offset of less than ± 1 μm [Fig. 5(c)]. If we set the offset to be 1 μm, the normalized value of optimal $|c_{92}|^2$ is decreased as the *NA* increases [Fig. 5(d)], but the coupling in this level of offset can still have a good efficiency (>85%) when the *NA* is around 0.95.

Optics EXPRESS

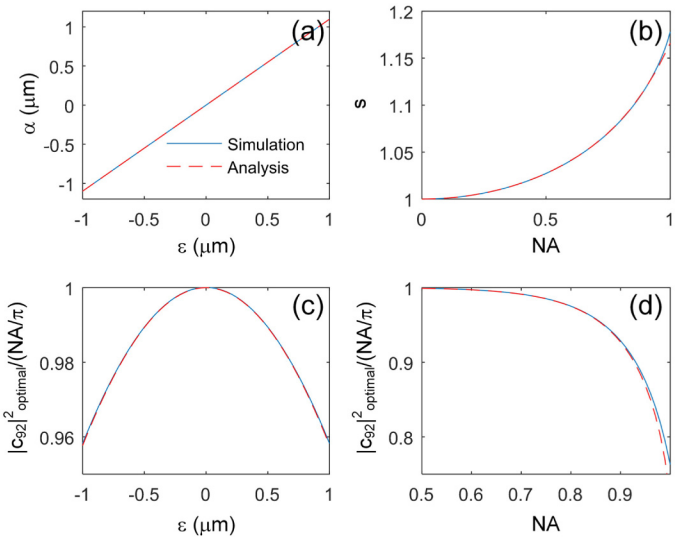

Fig. 5. Influence of the radius of the accelerating beams on the coupling efficiency ($m' = 92$ is under test). (a) Horizontal shift needed to allow the optimized coupling at different offsets of the radius with respect to the ideal case; (b) Slope of the linear relationship in (a) for different *NA*s, where the numerical values are obtained by a linear fitting in the range of ε in (a); (c, d) Optimized coupling efficiency for (c) various radius offsets when $NA = 0.85$ and (d) various *NA*s when the offset is set to be 1 μm.

4. Conclusion

In conclusion, we have analyzed free-space coupling to a cylindrical resonator by means of self-accelerating beams orbiting a semicircle, and we have found the best coupling condition. The analysis is further corroborated by simulation based on the theory derived and the computation via COMSOL software. Our theory shows that the optimal coupling efficiency can be linearly increased with the *NA* for these beams, much enhanced comparing to the case of Gaussian-like beams, particularly when larger *NA* and/or higher order azimuthal modes are under concern. Furthermore, the radius offset to the ideal case is also discussed. Since self-accelerating beams can de predesigned to propagate along any arbitrary convex trajectory, it is possible to reach a free-space coupling enhancement by applying these beams to deformed WGM resonators whose mode distribution is not necessarily circularly symmetric. Our results may prove useful for further experimental study on free space coupling via self-accelerating beams, which may offer a platform to study the fundamental physics and potential applications in WGM resonators [27–30], particularly in resonators made of droplets [27,28].

Funding

National Natural Science Foundation of China (NSFC) (11504186, 61575098, 91750204); The National Key R&D Program of China (2017YFA0303800); The 111 Project in China (B07013).

References

1. X. Fan and S. H. Yun, "The potential of optofluidic biolasers," Nat. Methods **11**(2), 141–147 (2014).
2. S. Kaminski, L. L. Martin, S. Maayani, and T. Carmon, "Ripplon laser through stimulated emission mediated by water waves," Nat. Photonics **10**(12), 758–761 (2016).
3. T. J. Kippenberg, R. Holzwarth, and S. A. Diddams, "Microresonator-based optical frequency combs," Science **332**(6029), 555–559 (2011).
4. W. Yu, W. C. Jiang, Q. Lin, and T. Lu, "Cavity optomechanical spring sensing of single molecules," Nat. Commun. **7**, 12311 (2016).

Optics EXPRESS

5. B. Matsko, A. A. Savchenkov, D. Strekalov, V. S. Ilchenko, and L. Maleki, "Review of applications of whispering-gallery mode resonators in photonics and nonlinear optics," IPN Progress Report **42**(162), 1–51 (2005).
6. Z. Ballard, M. D. Baaske, and F. Vollmer, "Stand-off biodetection with free-space coupled asymmetric microsphere cavities," Sensors (Basel) **15**(4), 8968–8980 (2015).
7. A. Giorgini, S. Avino, P. Malara, P. De Natale, and G. Gagliardi, "Fundamental limits in high-Q droplet microresonators," Sci. Rep. **7**(1), 41997 (2017).
8. N. Gaber, M. Malak, X. Yuan, K. N. Nguyen, P. Basset, E. Richalot, D. Angelescu, and T. Bourouina, "On the free-space Gaussian beam coupling to droplet optical resonators," Lab Chip **13**(5), 826–833 (2013).
9. C. L. Zou, F. J. Shu, F. W. Sun, Z. J. Gong, Z. F. Han, and G. C. Guo, "Theory of free space coupling to high-Q whispering gallery modes," Opt. Express **21**(8), 9982–9995 (2013).
10. C. Liu, A. Di Falco, D. Molinari, Y. Khan, B. S. Ooi, T. F. Krauss, and A. Fratalocchi, "Enhanced energy storage in chaotic optical resonators," Nat. Photonics **7**(6), 473–478 (2013).
11. C. Gmachl, F. Capasso, E. E. Narimanov, J. U. Nockel, A. D. Stone, J. Faist, D. L. Sivco, and A. Y. Cho, "High-power directional emission from microlasers with chaotic resonators," Science **280**(5369), 1556–1564 (1998).
12. G. D. Chern, H. E. Tureci, A. D. Stone, R. K. Chang, M. Kneissl, and N. M. Johnson, "Unidirectional lasing from InGaN multiple-quantum-well spiral-shaped micropillars," Appl. Phys. Lett. **83**(9), 1710–1712 (2003).
13. L. Wang, C. Wang, J. Wang, F. Bo, M. Zhang, Q. Gong, M. Lončar, and Y. F. Xiao, "High-Q chaotic lithium niobate microdisk cavity," Opt. Lett. **43**(12), 2917–2920 (2018).
14. X. F. Jiang, Y. F. Xiao, C. L. Zou, L. He, C. H. Dong, B. B. Li, Y. Li, F. W. Sun, L. Yang, and Q. Gong, "Highly unidirectional emission and ultralow-threshold lasing from on-chip ultrahigh-Q microcavities," Adv. Mater. **24**(35), 260–264 (2012).
15. S. X. Zhang, L. Wang, Z. Y. Li, Y. Li, Q. Gong, and Y. F. Xiao, "Free-space coupling efficiency in a high-Q deformed optical microcavity," Opt. Lett. **41**(19), 4437–4440 (2016).
16. Q. J. Wang, C. Yan, N. Yu, J. Unterhinninghofen, J. Wiersig, C. Pflügl, L. Diehl, T. Edamura, M. Yamanishi, H. Kan, and F. Capasso, "Whispering-gallery mode resonators for highly unidirectional laser action," Proc. Natl. Acad. Sci. U.S.A. **107**(52), 22407–22412 (2010).
17. J. Zhu, S. K. Özdemir, H. Yilmaz, B. Peng, M. Dong, M. Tomes, T. Carmon, and L. Yang, "Interfacing whispering-gallery microresonators and free space light with cavity enhanced Rayleigh scattering," Sci. Rep. **4**(1), 6396 (2015).
18. F. Shu, X. Jiang, G. Zhao, and L. Yang, "A scatterer-assisted whispering-gallery-mode microprobe," Nanophotonics **7**(8), 1455–1460 (2018).
19. Y. Hu, G. A. Siviloglou, P. Zhang, N. K. Efremidis, D. N. Christodoulides, and Z. Chen, Self-accelerating Airy beams: generation, control, and applications, in *Nonlinear photonics and novel optical phenomena*, Z. Chen and R. Morandotti, eds, (Springer, 2012), 1–46.
20. G. A. Siviloglou and D. N. Christodoulides, "Accelerating finite energy Airy beams," Opt. Lett. **32**(8), 979–981 (2007).
21. G. A. Siviloglou, J. Broky, A. Dogariu, and D. N. Christodoulides, "Observation of accelerating Airy beams," Phys. Rev. Lett. **99**(21), 213901 (2007).
22. I. Kaminer, R. Bekenstein, J. Nemirovsky, and M. Segev, "Nondiffracting accelerating wave packets of Maxwell's equations," Phys. Rev. Lett. **108**(16), 163901 (2012).
23. P. Zhang, Y. Hu, T. Li, D. Cannan, X. Yin, R. Morandotti, Z. Chen, and X. Zhang, "Nonparaxial Mathieu and Weber accelerating beams," Phys. Rev. Lett. **109**(19), 193901 (2012).
24. F. Courvoisier, A. Mathis, L. Froehly, R. Giust, L. Furfaro, P. A. Lacourt, M. Jacquot, and J. M. Dudley, "Sending femtosecond pulses in circles: highly nonparaxial accelerating beams," Opt. Lett. **37**(10), 1736–1738 (2012).
25. Y. Hu, D. Bongiovanni, Z. Chen, and R. Morandotti, "Multipath multicomponent self-accelerating beams through spectrum-engineered position mapping," Phys. Rev. A **88**(4), 043809 (2013).
26. P. Zhang, Y. Hu, D. Cannan, A. Salandrino, T. Li, R. Morandotti, X. Zhang, and Z. Chen, "Generation of linear and nonlinear nonparaxial accelerating beams," Opt. Lett. **37**(14), 2820–2822 (2012).
27. A. Giorgini, S. Avino, P. Malara, P. De Natale, M. Yannai, T. Carmon, and G. Gagliardi, "Stimulated Brillouin cavity optomechanics in liquid droplets," Phys. Rev. Lett. **120**(7), 073902 (2018).
28. Z. Feng and L. Bai, "Advances of optofluidic microcavities for microlasers and biosensors," Micromachines (Basel) **9**(3), 122 (2018).
29. X. Jiang, L. Shao, S. X. Zhang, X. Yi, J. Wiersig, L. Wang, Q. Gong, M. Lončar, L. Yang, and Y. F. Xiao, "Chaos-assisted broadband momentum transformation in optical microresonators," Science **358**(6361), 344–347 (2017).
30. L. Wang, C. Wang, J. Wang, F. Bo, M. Zhang, Q. Gong, M. Lončar, and Y. F. Xiao, "High-Q chaotic lithium niobate microdisk cavity," Opt. Lett. **43**(12), 2917–2920 (2018).